6834

Effects of Periodic Atmospheric Pressure Variation on Radon Entry into Buildings

Y. W. Tsang and T. N. Narasimhan

Radon is produced within the soil by the radioactive decay of radium, which is present in all earth-crustal materials, and is transported within the soil both by diffusion and advective flow of soil gas. At the soil-basement interface, radon enters buildings through restricted openings (cracks, joints, and holes). Existing data (Nazaroff et al., 1988; Nazaroff and Nero, 1988) indicate that high concentrations of indoor radon are usually associated with elevated influx rates of radon that is advectively transported with the bulk soil gas inflow. Current reasoning is that the bulk soil gas entry into buildings is driven by small pressure differentials (on the order of a few pascals) between the basement and the outside atmosphere. The pressure differences are caused by indoor-outdoor temperature differences, interaction of wind with the building envelope, and operation of exhaust fans.

It is known that the transient barometric pressure fluctuations consist of periodic components with amplitudes ranging from a few pascals for periods of minutes to a few hundred pascals in diurnal variations. Since these transient pressure variations have magnitudes far larger than the pressure difference responsible for steady airflow, the question arises as to the effect of the atmospheric pressure pumping on radon entry rate into buildings. Here we report the results of our investigation (Tsang and Narasimhan, 1992) on the transport of radon by soil gas into building basements during periodic variations in barometric pressure.

MODELING STUDIES

To study the combined effects of barometric fluctuations and constant underpressure on soil gas inflow and radon entry at a basement, we define the problem as shown schematically in Figure 1. The water table lies 5 m below the land surface and 3 m below the 10-m-wide basement floor. In the absence of all driving forces except gravity, the soil air within the soil formation will be static if the gas

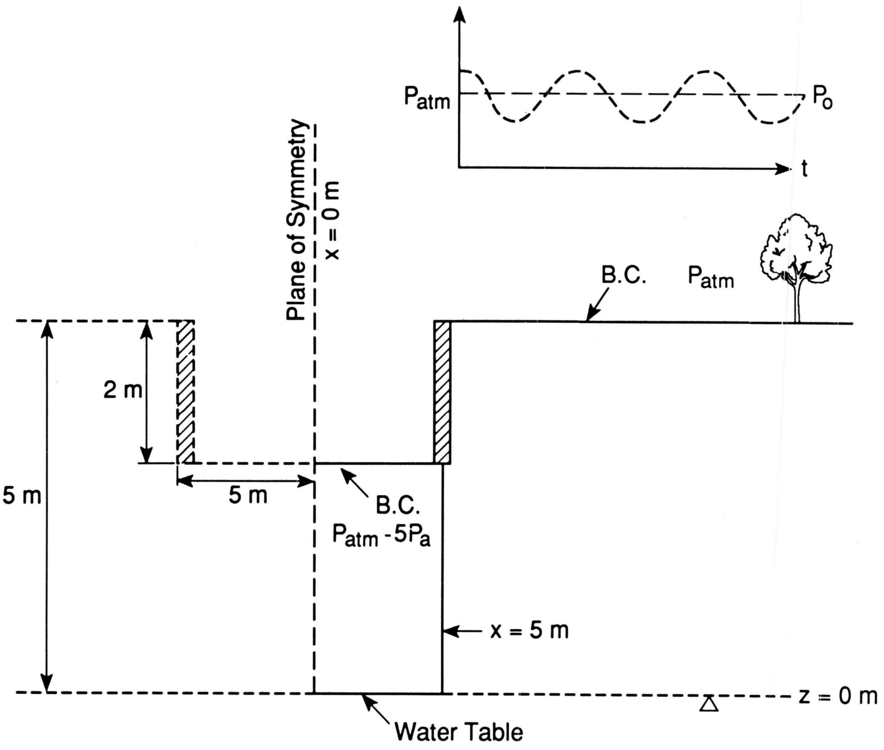

Figure 1. Schematic diagram for the basement configuration and pressure boundary conditions for modeling radon entry. [XBL 899-3439]

pressure at each elevation, z, above the water table is $P_0(z) = \overline{P}_{wt} - \rho g z$, where $\overline{P}_{wt}$ is the mean air pressure at the water table (assumed throughout this work to be 10^5 Pa), ρ is the density of air, and g is acceleration due to gravity. Pressure boundary conditions that would induce persistent air inflow into the basement were chosen as follows. The mean pressure $\overline{P}$ at the land surface is equal to P_0 (z = 5 m), and the mean pressure at the basement floor is assumed to be always 5 Pa below that corresponding to the pneumostatic state, P_0 (z = 3 m) – 5 Pa, thus ensuring a continuous Darcy flow of soil gas into the basement. The fluctuations in the atmospheric pressure are assumed to be felt at both the land surface and at the basement floor with no damping or phase lag. For our initial studies, the atmospheric pressure fluctuations are assumed to consist of a single sinusoidal component with a given amplitude and frequency, oscillating around the respective mean values of $\overline{P}$ at the outside land surface and the basement. Two frequencies with representative values of amplitudes (based on a Fourier decomposition of barometric pressure data) are chosen in this study to investigate the dependence of air flow and radon entry on barometric pressure pumping. They are (1) a short period of T = 0.5 hr with pressure amplitude A = 50 Pa and (2) a diurnal variation with a 24-hr period and the typical pressure amplitude of 250 Pa.

Two boundary conditions at the basement floor are implemented. One is an open boundary over the entire floor; this corresponds to a basement with no impermeable covering such as a concrete slab, referred hereafter to as the dirt floor basement. The other is a closed boundary, except for a 1-cm opening centered at x = 4.4 m (0.6 m from the basement edge); this corresponds to a basement covered by an "impermeable" concrete slab except for small penetrations (cracks, joints, holes) that extend between the indoors and the soil.

For our calculations we use an isothermal, multidimensional fluid flow and chemical transport model CHAMP (Narasimhan et al., 1985). We idealize the configuration shown in Figure 1 as a two-dimensional XZ planar region with a unit thickness in the third dimension Y. We consider a simplified system where the permeability is assumed not to vary with distance from the water table, and in most cases a homogeneous soil formation is assumed, where modeling studies are carried out with permeabilities ranging from 10^{-13} m^2 to 10^{-10} m^2 for both the dirt floor basement configuration as well as the impermeable basement floor with a 1-cm crack configuration. The only type of permeability heterogeneity considered in this study is the special case where a thin layer immediately below the basement floor has a permeability a few orders of magnitude larger than the rest of the soil formation. This corresponds to the physical situation where a porous sublayer of highly permeable aggregate is present below the basement floor. The permeability value chosen for this high-permeability layer of thickness $\Delta z = 0.4$ m is 10^{-10} m^2. For the radon source in soil, we assume a uniform production rate of 0.1836 Bq/m^3-s, per unit volume of soil gas, with a decay constant of 2.1×10^{-6}/s, which corresponds to the radon half-life of 3.8 days. The coefficient of diffusion of radon in soil, corrected for soil porosity and tortuosity effects, is chosen to be 1×10^{-6} m^2/s.

RESULTS—RADON ENTRY INTO A BASEMENT

Figure 2 shows (1) the time-varying oscillatory radon entry rate (the top four curves with reference to units on the left ordinate) for the basement with the 1-cm crack configuration when the forcing function has a period of 0.5 hr and (2) the sinusoidal time variation of the pumping pressure (bottom curve with reference to units on the right ordinate). Radon fluxes are shown for two cases: $k = 10^{-10}$ m^2 (solid curve) and $k = 10^{-11}$ m^2 (broken curve). The steady rates of radon entry into the basement in the absence of pressure pumping are represented by the two horizontal lines at –0.52 Bq/s (for $k = 10^{-10}$ m^2) and –0.075 Bq/s (for $k = 10^{-11}$ m^2). The negative sign attached to the radon fluxes simply indicates that the direction of radon flux is into the basement. The pressure increases in the first half of the 0.5-hr period, causing the air to flow from the basement back into the soil formation. In the modeling, we impose at the basement the boundary condition that the radon concentration is zero; this is based on the implicit assumption that the air in the basement is quickly mixed to dilute the influx of radon. Hence the air that is flowing back from the basement into the soil formation effectively carries no radon, thus forcing the advective

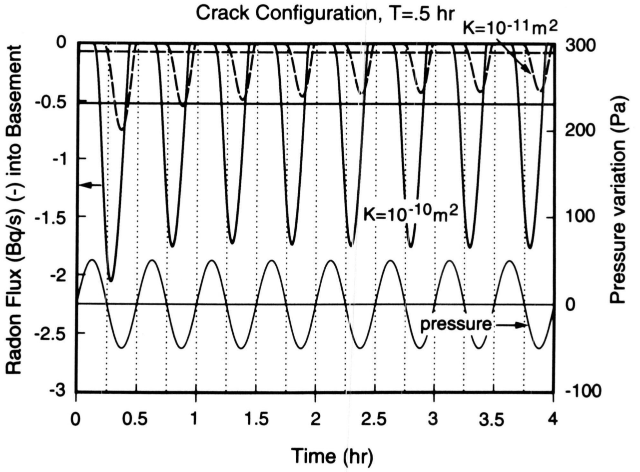

Figure 2. Radon inflow into a basement crack with and without pressure pumping of $T = 0.5$ hr for permeabilities 10^{-10} and 10^{-11} m^2 and pressure variation. [XBL 9110-6109]

radon flux to go to zero for the first part of the pumping period in Figure 2. Figure 2 displays the total radon flux, which includes both the advective and diffusive contributions; the fact that in the first part of the pumping cycle the total inflow practically reduces to zero indicates that the steady-state radon flow is dominated by advective flux and that there is negligible contribution from the diffusive radon flow. During the second part of the 0.5-hr pumping period, the pressure decreases below its mean value, hence the air flow from the soil column into the basement increases, carrying with it additional advective radon. If the radon flux is exactly in phase with the pumping pressure, then the radon entry will decrease for the first half and then increase for the second half of the pumping period. Note that, instead, there is a phase lag between the radon flow and the pressure variation. The total amount of radon entry into the basement for the cases with or without pressure pumping is compared by the estimated area enclosed by the radon flux curve and the axis $x = 0$ in each period. Let the area enclosed by the horizontal line of the steady-state radon flux and the axis $x = 0$ be A_1, and let the area enclosed by the oscillatory radon flux and the axis $x = 0$ be A_2. The percent increase in radon entry is defined as $[(A_2 - A_1)/A_1] \times 100$ and is given in Table 1.

The simulation results for the 1-cm crack configurations are summarized in Table 1. Table 1 is organized as follows. The first column specifies the absolute permeability, the second through fourth columns relate to soil gas flow, and the fifth through eighth columns relate to radon entry. In particular, the second column gives the steady-state soil air flow into the basement; that is, the air flux with only the –5 Pa of underpressure at the basement (in the absence of sinusoidal pressure pumping). With the sinusoidal pressure pumping, the air flux becomes oscillatory in time about the steady-state value. Columns 3 and 4 list the ratio of the amplitude of the oscillatory soil air flow to the steady-state value for the pumping periods of 0.5 and 24 hr, respectively. The fifth column lists the steady state total radon flux into the basement, including both the advective and diffusive contributions. The sixth column gives contributions from only the diffusive radon flow into the basement; that is, the influx of radon in the absence of all pressure differences. The diffusive flux is of course independent of the permeability. The seventh and eighth columns list, respectively, the percentage increase in radon entry (with reference to column 5) into the basement from sinusoidal pressure pumping with oscillatory periods of 0.5 and 24 hr and amplitudes of 50 and 250 Pa. Since the radon flux at the basement is oscillatory under the influence of pressure pumping, the percentage increase in radon entry over the constant steady-state value are time averages, as discussed earlier.

Columns 5 through 8 of Table 1 list the radon entry into the basement. In column 5, the steady-state radon flow is dominated by the diffusion process in the lowest-permeability case studied: (10^{-13} m^2); for the other cases, the steady radon inflow increases as permeability increases because of the advective process. We note that the increase of radon entry into the basement due to atmospheric pumping is not directly proportional to the soil permeability. With a high-permeability soil, there is large enhancement of radon inflow during that part of the cycle when the pumping pressure is decreasing, yet the radon inflow into the basement is forced to zero when the pressure is increasing. The steady-state radon inflow from the basement depressurization alone in the absence of pumping also increases with permeability. Consequently the relationship between permeability and increase in radon entry is complex. It is in the intermediate permeability range that the

Table 1. Air flow and radon entry at a basement crack with constant underpressure of 5 Pa in the absence or presence of barometric pumping.

Soil k (m^2)	Air flux (kg/s)			Radon entry (Bq/s)			
	Steady state	Ratio of oscillatory amplitude to steady state		Steady state		Percent increase of radon entry with pressure pumping	
		$T = 0.5$ hr $A = 50$ Pa	$T = 24$ hr $A = 250$ Pa	Diffusive + advective	Diffusive alone	$T = 0.5$ hr $A = 50$ Pa	$T = 24$ hr $A = 250$ Pa
10^{-10}	0.107×10^{-4}	2.9	0.3	0.520	0.011	10	0.5
10^{-11}	0.107×10^{-5}	12	3.1	0.075	0.011	38	6
10^{-12}	0.107×10^{-6}	15	28	0.015	0.011	31	120
10^{-12*}	0.259×10^{-6}	29	28	0.022	0.011	78	190
10^{-13}	0.107×10^{-7}	17	64	0.011	0.011	1	32
10^{-13*}	0.263×10^{-7}	41	131	0.012	0.011	31	198

*With a 0.4-m thick layer of aggregate ($k = 10^{-10}$ m^2) beneath the basement slab.

largest percentage increase in radon entry over time is found. This is the case when the steady-state radon inflow is not too large yet there is appreciable enhancement in advective radon inflow when the pressure is decreasing. The largest predicted increases (for uniform soil permeability) are for the cases $k = 10^{-11}$ m^2 and $T = 0.5$ hr in the dirt basement configuration and $k = 10^{-12}$ m^2 and $T = 24$ hr in the crack configuration. Table 1 shows that the increase in radon inflow is even greater if a high-permeability (10^{-10} m^2) layer is present beneath the concrete slab. This kind of permeability heterogeneity maximizes the effect of the "local" enhancement of the pumping advective radon transport at the basement opening, yet the effective permeability of the total soil mass remains small, since the high-permeability layer constitutes only a small fraction of the total volume; the small effective permeability ensures that steady-state radon inflow due to basement depressurization remains small if the soil permeability is $\leq 10^{-12}$ m^2.

SUMMARY AND CONCLUSION

Study results show that for a homogeneous soil medium, the largest increase in radon entry (over steady-state advective transport with a 5-Pa underpressure at the basement) occurs for $k = 10^{-12}$ m^2 with the barometric variation of period $T = 24$ hr and amplitude 250 Pa in the crack configuration. The increase is 120%. In the dirt floor configuration, the largest percentage increase is 68% over that of steady radon entry with 5 Pa underpressure at the basement for $k = 10^{-11}$ m^2 and a pumping period of 0.5 hr. The increase in radon entry with pumping is further enhanced when there is a heterogeneity in permeability arising from the physical situation of a high-permeability aggregate layer immediately below the basement floor.

The different configurations chosen (dirt floor basement and impermeable basement floor with crack) serve to demonstrate the relative importance of the different transport processes: diffusive, steady-state advective, and pressure-pumping advective. A significant result from this study is that the advective radon transport from pressure pumping may be an order of magnitude larger than the diffusive transport in the absence of a persistent underpressure at the basement, for $k = 10^{-10}$ m^2. This may help to explain indoor radon concentrations during periods of low steady-state driving force.

ACKNOWLEDGMENT

We would like to thank Mohsen Alavi of the Earth Sciences Division of LBL for help in modifying the computer code CHAMP.

REFERENCES

Narasimhan, T.N., Alavi, M., Liu, C.W., 1985. CHAMP—A computer code for modeling transient fluid flow and chemical transport with hydrodynamic dispersion in variably saturated systems. *In* Proceedings of the Symposium on Groundwater Flow and Transport Modeling for Performance Assessment of Deep Geologic Disposal of Radioactive Waste: A Critical Evaluation of the State of the Art. Albuquerque, New Mexico, May 20–21.

Nazaroff, W.W. and Nero, A.V., Jr. (eds.), 1988. Radon and Its Decay Products in Indoor Air. Wiley, New York, p. 57–111.

Nazaroff, W.W., Moed, B.A., and Sextro, R.G., 1988. Soil as a source of indoor radon: Generation, migration, and entry. *In* W.W. Nazaroff and A.V. Nero, Jr. (eds.), Radon and Its Decay Products in Indoor Air. Wiley, New York, p. 57–111.

Tsang, Y.W., and Narasimhan, T.N., 1992. Effects of periodic atmospheric pressure variation on radon entry into buildings. J. Geophys. Res., v. 97, no. B6, p. 9161–9170.

6835

Studies of the Role of Fault Zones on Fluid Flow Using the Site-Scale Numerical Model of Yucca Mountain

C. S. Wittwer, G. Chen, and G. S. Bodvarsson

Lawrence Berkeley Laboratory (LBL) in cooperation with the United States Geological Survey (USGS) has developed a three-dimensional site-scale numerical model of the unsaturated zone at Yucca Mountain, Nevada. The hydrogeology of the site is controlled by fluid flow through heterogenous, unsaturated fractured and porous layers of volcanic tuffs in an arid environment. The site-scale model covers an area of about 30 km^2 around the potential repository area and is bounded by major fault zones to the north (Yucca Wash fault), east (Solitario Canyon fault), and west (Bow Ridge fault). The numerical grid was designed to account for the geological and hydrogeological mechanisms that have been described in the literature as being relevant to moisture flow at Yucca Mountain (Montazer